Néel ''orange-peel'' coupling in magnetic tunneling junction devices

B. D. Schrag,[a] A. Anguelouch, S. Ingvarsson, and Gang Xiao
Department of Physics, Brown University, Providence, Rhode Island 02912

Yu Lu, P. L. Trouilloud, A. Gupta, R. A. Wanner, and W. J. Gallagher
IBM T. J. Watson Research Center, Yorktown Heights, New York 10598

P. M. Rice and S. S. P. Parkin
IBM Almaden Research Center, San Jose, California 95120

We present measurements of the magnitude of Néel ''orange-peel'' coupling due to interface roughness in a series of magnetic tunneling junction devices. Results from magnetometry and transport measurements are shown to be in good agreement with the theoretical model of Néel. In addition, we have used transmission electron microscopy to directly probe the sample interface roughness and obtain results consistent with the values obtained by magnetometry and transport methods. © *2000 American Institute of Physics.* [S0003-6951(00)00541-6]

Due to their great technological promise as potential memory elements and magnetic sensors, magnetic tunneling junctions (MTJs) have been extensively studied[1–3] by many academic and industrial groups over the past five years. One of the technological hurdles, which must be dealt with when considering such applications, is that of interlayer magnetic coupling between the electrodes. It is of importance that any stray magnetic fields affecting the free ferromagnetic layer be eliminated. It has been previously shown[4,5] that two separate effects tend to produce extraneous magnetic fields in the plane of the free layer: magnetostatic coupling due to uncompensated poles near the edges and Néel ''orange-peel'' coupling due to interface roughness, both of which originate in the pinned layer. In this work, we study and quantify the latter effect in MTJs by a variety of methods: directly, via the technique of magnetometry and via magnetotransport measurements,[5,6] and indirectly, by imaging analysis of transmission electron microscope (TEM) cross-sectional images of the MTJ layer structure.

We studied twelve different samples, all fabricated during the same sputtering run and with the same layer composition: Si(100) substrate /Ta/Al/NiFe/FeMn/Co(*P2*)/Ru/ Co(*P1*) (pinned)/Al$_2$O$_3$(barrier)/NiFe(free)/Al/Ta. However, the thickness of the barrier, free, and pinned layers varied from sample to sample. Figure 1 shows a representative TEM cross-sectional image of one of our samples, with layer thicknesses labeled.

Measurements of junction resistance in a two-dimensional applied magnetic field were conducted as described previously.[5,6] These measurements were done on chips patterned into many rectangular junctions with dimensions on the order of microns. The resistance versus field curves correspond directly to the magnetic hysteresis loop of the free layer, allowing us to extract the magnetic switching fields and bias fields of the free layer. The advantage of this method is that important magnetic parameters can be obtained, regardless of how small the free electrode is. For bulk

magnetic tunneling junctions, we also used vibrating sample magnetometry (VSM) to measure the switching fields and bias fields of the free layers. Twelve different bulk samples were examined this way.

Magnetic interlayer coupling is significant in MTJs because of the close proximity of the two magnetic electrodes. Figure 2 is a schematic showing the interface roughness and the fields due to magnetostatic (H_M) and Néel (H_N) couplings. It has been shown by us[5,6] that while magnetostatic coupling is not negligible for samples of this size, it is possible to separate the two forms of coupling by measuring junctions of varying sizes. From these measurements, we obtained the interface roughness parameters from the Néel field strengths. In the model of Néel, a sinusoidal roughness profile is assumed, and the orange-peel coupling field is given by

$$H_N = \frac{\pi^2}{\sqrt{2}}\left(\frac{h^2}{\lambda t_F}\right)M_S \exp(-2\pi\sqrt{2}t_s/\lambda), \qquad (1)$$

where h and λ are the amplitude and wavelength of the roughness profile (see Fig. 2), t_F and t_s are the thickness of the free layer and that of the barrier, and M_S is the magnetization of the free layer.
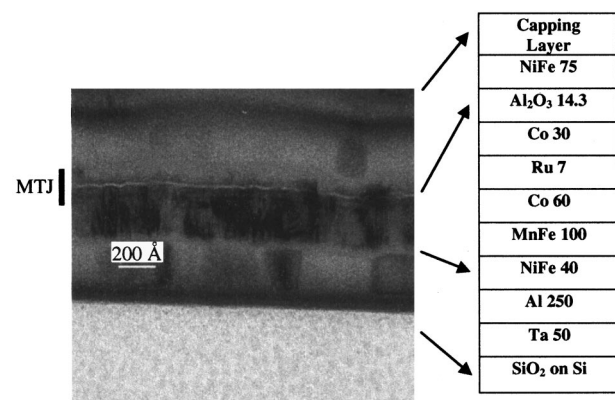

| Capping Layer |
| NiFe 75 |
| Al$_2$O$_3$ 14.3 |
| Co 30 |
| Ru 7 |
| Co 60 |
| MnFe 100 |
| NiFe 40 |
| Al 250 |
| Ta 50 |
| SiO$_2$ on Si |

FIG. 1. TEM cross-sectional image and layer structure of one representative sample. Layer thicknesses are given in angstroms.

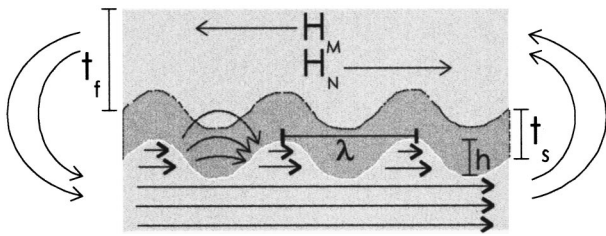[a]Electronic mail: schrag@baras.physics.brown.edu

FIG. 2. Schematic depicting the two dominant interlayer coupling mechanisms.

The inset of Fig. 3 shows a representative hysteresis loop in a bulk sample. It is noted that only Néel coupling exists in a bulk sample, and magnetostatic coupling is zero. The field scale used is small enough that only the free layer experiences substantial changes in magnetization. In analyzing the VSM data, we assumed that the switching field could be approximated by the field at which the resistance value was equal to one half of the maximum observed magnetoresistance. For each sample, we extrapolated the coordinates of the two points at which the experimental curves crossed through this resistance value. These two points were then averaged to obtain an approximate Néel coupling field strength, which is shown in Fig. 3 as a function of the barrier thickness (t_s) for three series of samples with different free layer thickness (t_F). The three solid lines are the best fits of Eq. (1) to the experimental data. The obtained roughness amplitude (h) and wavelength (λ) are listed in Table I. It can be seen that all experimental data are accounted for by the Néel equation.

The Néel coupling fields can also be obtained via resistance versus field measurements on patterned micron-sized MTJs.[5,6] Using Eq. (1), we can also extract the roughness

TABLE I. Summary of interface roughness parameters for each experimental approach.

Method	h (Å)	λ (Å)
transport	7.3±0.5	94±15
VSM	7.1±0.3	100±10
TEM	10.1±3.8	101±8

amplitude and wavelength. The results are shown in Table I, which reveals that the VSM and magnetotransport measurements give consistent roughness parameters within the experimental errors.

To further confirm the roughness parameters, we conducted an analysis of cross-sectional TEM images (see Fig. 1). From the TEM micrograph, we were able to extract the roughness magnitude and wavelength for the barrier interface as follows. First, the image was converted into data points relating the vertical position of the barrier interface as a function of the horizontal distance along the sample. These data were then smoothed and the positions of all local maxima and minima were recorded. Then, the coordinates of adjacent minima and maxima were used to extract an effective magnitude and wavelength corresponding to that pair of points. This process was repeated for about 200 peaks and valleys. These data were then plotted in two histograms and fitted to log-normal distributions:

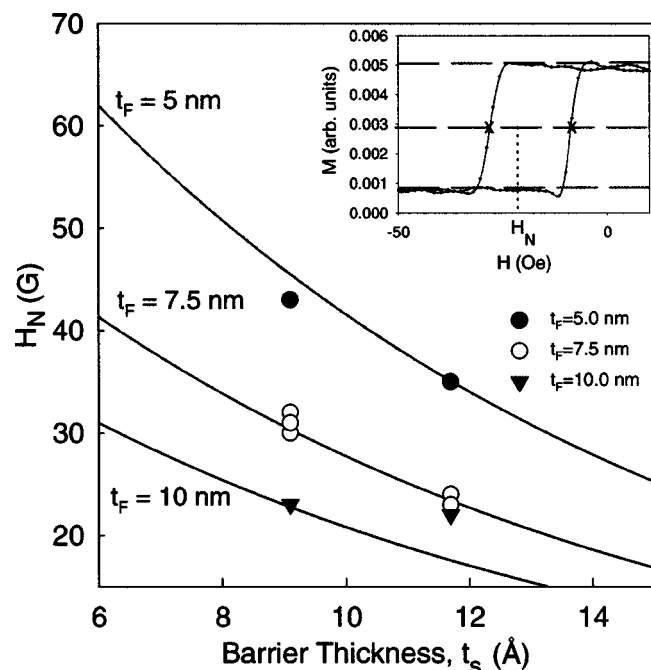$$P(x) = \frac{1}{\sqrt{2\pi}\sigma} \exp\left(\frac{-(\ln x - \mu)^2}{2\sigma^2}\right), \qquad (2)$$

FIG. 3. Orange-peel coupling field values extrapolated from VSM measurements. Solid lines are a fit to the data for different free layer thicknesses. Inset: sample VSM hysteresis loop showing the magnetic reversal of the free layer. The top and bottom dashed lines indicate the saturation magnetization levels of the free layer while the intermediate line denotes the ''half-switched'' state used to extrapolate the Néel field H_N.
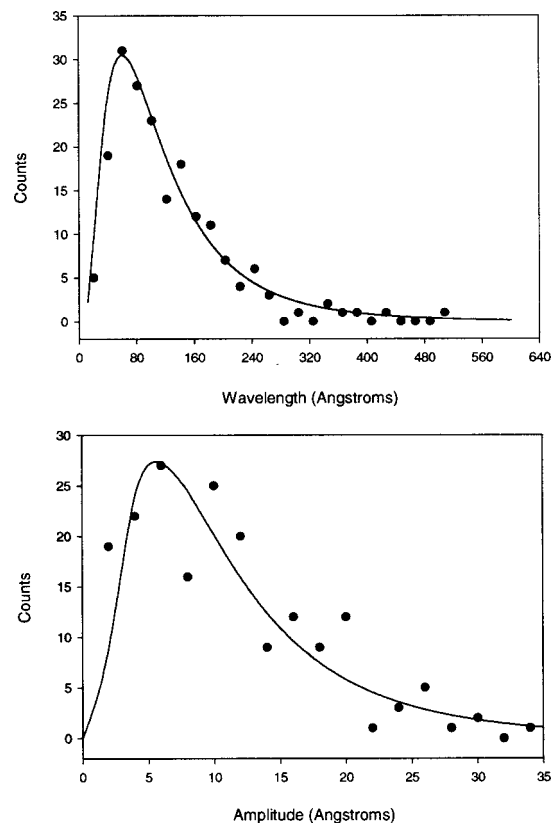

FIG. 4. Histograms indicating the distribution of fitted wavelengths and amplitudes of the tunneling barrier peaks from digitized TEM pictures. Solid lines are log-normal fits to the data. Parameters from these fits were used to get direct estimates of roughness parameters.

Appl. Phys. Lett., Vol. 77, No. 15, 9 October 2000

Schrag *et al.* 2375

where u and σ are measures of the mean and standard deviation of the distribution. These fits are represented by solid lines in Fig. 4. The fitted values of μ for each histogram were used to give approximate values for the effective wavelength and amplitude of the roughness for the sample in question (see Table I). Because of the asymmetry of the log-normal function, the peaks of the histograms do not correspond exactly to these values.

A summary of the results for each experimental technique is shown in Table I. It can be seen that the results are quite consistent. The roughness wavelength obtained is similar to those given in studies of spin-valve systems,[7,8,9] and is most likely determined by the intrinsic grain sizes. The only discrepancy lies in the roughness magnitude calculated using the TEM images. This value is larger than the results from the other methods. There are two large sources of uncertainty in this calculation. First of all, the pixel size of the TEM images was 2 Å. Second, the assumption of a uniform sinusoidal roughness required to apply the model of Néel creates an error whose magnitude was approximated by the half-width of the log-normal fit to the data shown in Fig. 4. By this measure, the uncertainty in the magnitude is ± 3.8 Å, which makes our value consistent to within experimental error. In order to use direct TEM images to calculate Néel coupling more accurately, it will probably require abandoning the assumption of sinusoidal roughness and using magnetostatic methods to calculate offset fields from actual roughness patterns. However, we believe that our results are accurate enough to allow researchers and engineers to predict and control orange-peel coupling in new MTJ devices.

In summary, we have used three independent experimental techniques to probe the Néel coupling of magnetic tunneling junction devices. We have obtained the magnitude and wavelength of the idealized sinusoidal interface roughness in each case and have found all of our values to be consistent. We believe that these results will facilitate better design of MTJ-based devices.

[1] J. S. Moodera, L. R. Kinder, T. M. Wong, and R. Meservey, Phys. Rev. Lett. **74**, 3273 (1995); J. Appl. Phys. **79**, 4724 (1996).

[2] N. Tezuka and T. Miyazaki, J. Appl. Phys. **79**, 6262 (1996); J. Magn. Magn. Mater. **139**, L231 (1995).

[3] W. J. Gallagher, S. S. P. Parkin, Y. Lu, X. P. Bian, A. Marley, K. P. Roche, R. A. Altman, S. A. Rishton, C. Jahnes, T. M. Shaw, and G. Xiao, J. Appl. Phys. **81**, 3741 (1997).

[4] K.-S. Moon, R. E. Fontana, Jr., and S. S. P. Parkin, Appl. Phys. Lett. **74**, 3690 (1999).

[5] A. Anguelouch, B. D. Schrag, G. Xiao, R. Wanner, P. Trouilloud, Y. Lu, W. J. Gallagher, and S. S. P. Parkin, Appl. Phys. Lett. **76**, 622 (2000).

[6] B. D. Schrag, A. Anguelouch, G. Xiao, P. Trouilloud, Y. Lu, W. J. Gallagher, and S. S. P. Parkin, J. Appl. Phys. **87**, 4682 (2000).

[7] L. Néel, C. R. Acad. Sci., Paris, **255**, 1676 (1962).

[8] Th. G. S. M. Rijks, R. F. O. Reneerkens, R. Coehoorn, J. C. S. Kools, M. F. Gillies, J. N. Chapman, and W. J. M. de Jonge, J. Appl. Phys. **82**, 3442 (1997).

[9] J. C. S. Kools, W. Kula, D. Mauri, and T. Lin, J. Appl. Phys. **85**, 4466 (1999).